Atmos. Chem. Phys. Discuss., 10, 9695–9729, 2010
www.atmos-chem-phys-discuss.net/10/9695/2010/

Atmospheric Chemistry and Physics Discussions

Heterogeneous freezing of water droplets containing kaolinite and montmorillonite particles

B. J. Murray[1], **T. W. Wilson**[1], **S. L. Broadley**[1], **and R. H. Wills**[1,*]

[1]School of Chemistry, Woodhouse Lane, University of Leeds, Leeds LS2 9JT, UK
[*]now at: Department of Chemistry, University of Warwick, Gibbet Hill Road,
Coventry CV4 7AL, UK

Received: 1 April 2010 – Accepted: 9 April 2010 – Published: 16 April 2010

Correspondence to: B. J. Murray (b.j.murray@leeds.ac.uk)

Published by Copernicus Publications on behalf of the European Geosciences Union.

Abstract

Clouds composed of both ice particles and supercooled liquid water droplets exist at temperatures above ~236 K. These mixed phase clouds, which strongly impact climate, are very sensitive to the presence of solid particles that can catalyse freezing. In this paper we describe experiments to determine the rate at which kaolinite and montmorillonite nucleate ice when immersed within water droplets. These are the first immersion mode experiments in which the ice nucleating ability of individual minerals has been determined quantitatively. Water droplets containing a known amount of clay mineral were supported on a hydrophobic surface and cooled at a rate of 10 K min^{-1}. The temperatures at which individual 10–40 µm diameter droplets froze were determined by optical microscopy. As the concentration of kaolinite in the droplets was increased from 0.005 wt% to 1 wt% the median nucleation temperature increased from close to the homogeneous nucleation limit (236 K) to 240.8±0.6 K. We go onto show that the probability of freezing scales with surface area of the kaolinite inclusions rather than, as is often assumed, the volume of the droplet. When droplets contained montmorillonite ice always nucleated at 245.8±0.6 K, independent of the mineral concentration. We report temperature dependent nucleation rates and present parameterisations for nucleation by these minerals which capture the surface area and cooling rate dependence of the nucleation rate. We show that our parameterisations produce significantly different results to parameterisations employed in global models. These results also highlight the importance of understanding the ice nucleating properties of individual minerals rather than complex mixtures of minerals found in natural dusts and so-called test dusts.

1 Introduction

In the absence of appropriate ice nuclei, cloud water droplets will supercool to ~236 K at which temperature they spontaneously freeze. The presence of suitable solid particles, known as ice nuclei, can catalyse ice formation at much higher temperatures. Ice nuclei tend to be rare in comparison to cloud condensation nuclei (DeMott et al., 2003a) and ice particles resulting from heterogeneous nucleation grow at the expense of any unfrozen droplets. This results in a shift to lower number densities of larger particles which has a profound impact on cloud lifetimes and radiative properties as well as precipitation (Pruppacher and Klett, 1997; Lohmann and Feichter, 2005). Hence, a fundamental understanding of ice nucleation in atmospherically relevant droplets is key for quantifying the role of clouds in the climate system and the hydrological cycle.

Heterogeneous freezing can occur in four different modes: deposition nucleation, condensation freezing, immersion freezing, and contact freezing (Pruppacher and Klett, 1997). Deposition nucleation occurs when vapour adsorbs onto a solid surface and is transformed into ice, but is thought to be less important than the other mechanisms in mixed phase clouds (Lohmann and Diehl, 2006). However, deposition nucleation is thought to be important in upper tropospheric ice clouds (Murray et al., 2010b; DeMott, 2002). Immersion freezing occurs when ice nucleates on a solid particle immersed in a supercooled liquid droplet, whereas condensation freezing occurs when water vapour condenses on a solid particle and then freezes. The distinction between immersion and condensation modes is subtle, since the most likely route for immersing a particle inside a droplet is through condensation on that particle. Contact freezing occurs when a solid particle collides with a supercooled liquid droplet, resulting in ice nucleation (Vali, 1985; Pruppacher and Klett, 1997). Immersion mode and contact freezing are thought to be most important in mixed phase clouds (Lohmann and Diehl, 2006).

The identity, concentration, global distribution and the efficiency with which potential ice nuclei catalyse ice formation are all poorly quantified at present. Mineral dust is known to be an important class of ice nuclei and is transported many thousands of miles from arid source regions (DeMott et al., 2003b; Sassen, 2005). On the order of 10^{15} g of dust particles with diameters less than 10 µm are injected into the Earth's atmosphere per annum from surface sources such as deserts (Denman et al., 2007).

Approximately 50% of the dust from Asia is transported as far as the Pacific and continental USA (Zhang et al., 1997). African dust is known to be transported over the Atlantic and is found in the Caribbean (Usher et al., 2003; Glaccum and Prospero, 1980) and 40 million tons of African dust is transported annually to the Amazon basin where it acts as an important fertiliser (Koren et al., 2006). Furthermore, there has been a two to four fold increase in airborne mineral dust in the North Atlantic region since the 1960s and this is possibly linked to human activities (Mahowald and Kiehl, 2003).

Ice nucleation on mineral dust is known to impact cloud formation on a planetary scale, but its quantitative impact on climate and precipitation remains poorly defined (Denman et al., 2007). Mineral dust suspended in the Earth's atmosphere is made up of a range of minerals (Glaccum and Prospero, 1980; Kandler et al., 2007); however the ice nucleating potential of individual minerals is poorly characterised. Early studies where residues of snowflakes were analysed by electron microscopy demonstrated that clay minerals were present inside 28 to 88% of snowflakes, depending on location (Pruppacher and Klett, 1997). More recently, single particle mass spectrometry has shown that mineral dusts and metallic particles are substantially enhanced in the fraction of aerosol that nucleate ice heterogeneously, relative to the background aerosol (DeMott et al., 2003a, b; Richardson et al., 2007; Mertes et al., 2007; Pratt et al., 2009). Richardson et al. (2007) demonstrated that mineral dust represented only a few percent of the total background aerosol, but represented ∼1/3 of the particles that served as ice nuclei in mixed phase clouds. Prenni et al. (2009) showed that ice nucleation on mineral dust becomes increasingly important below 246 K in the Amazon region where ice nucleation is dominated by biogenic material above 248 K.

Some progress in modelling the climate impacts of cloud glaciation is being made. In the first global modelling sensitivity study of its kind, Lohmann and Diehl (2006) studied the impact of two clay minerals on stratiform mixed phase clouds and found the radiative forcing to be between 1.0 and 2.1 W m^{-2}. Hence radiative forcing by mineral dust through ice nucleation in just one cloud type is comparable to the forcing by anthropogenic CO_2 (1.7 $W\,m^{-2}$). In addition, Lohmann and Diehl (2006) demonstrated that there is a strong sensitivity to dust type, of 1.1 $W\,m^{-2}$, in going from montmorillonite to kaolinite. The parameterisation of immersion mode nucleation Lohmann and Diehl (2006) used in their global modelling study was based on experimental data reported in the 1960s (Hoffer, 1961) and 1970s (Pitter and Pruppacher, 1973). In neither of these papers was the quantity or surface area of mineral dusts present in their droplets reported and the nucleation temperatures quoted for the same minerals varied by 5–10 K between the papers. While the modelling work of Lohmann and Diehl is intriguing, it must be borne in mind that the fundamental data on which their work is based needs to be improved.

In this paper we present measurements of the efficiency with which the clay minerals kaolinite and montmorillonite nucleate ice when immersed in water droplets. We show that nucleation rates on kaolinite scale with the surface area of the solid inclusion, but ice nucleation on montmorillonite does not. We go on to present the data in a way which will be useful in modelling studies.

2 Methodology

The equipment used to make these measurements has been described previously (Murray et al., 2010a). Briefly, the droplets were supported on a hydrophobic surface positioned on a home made cold stage which was coupled to a commercial optical transmission microscope with a 10× objective. For these experiments we cooled to 228 K at a rate of 10 $K\,min^{-1}$. Droplet freezing temperatures were determined from digital images of the experiments which were recorded using a camera coupled to the microscope.

In order to measure ice nucleation quantitatively, special care was taken in generating the droplets. Droplets containing a known quantity of mineral dust were produced using a home made nebuliser similar in design to one used in the past (Pant et al., 2006). The nebuliser did not become blocked by clay particles for the range of concentrations of the dust-in-water suspensions used in these experiments. The concentration of dust in the suspensions was determined gravimetrically and the dust was suspended by mixing for at least 12 h with a magnetic stirring bead. We did not use more vigorous mixing methods, such as high speed mixers or sonic baths, in order to minimise modification of the dust grains. The water we used has a resistance of 18.2 MΩ.

The suspensions were nebulised into a chamber which was maintained at saturation by means of an additional saturated flow of nitrogen gas. This ensured that the droplets did not grow or shrink through evaporation or condensation once they exited the nebuliser. We assumed that the mineral dust concentration was fixed at the value of the original suspension. Droplets were then allowed to settle onto a coated glass cover slip which was placed within the chamber. The borosilicate glass cover slip was coated with a hydrophobic organosilane. This substrate had a contact angle of 100°, and ensured the surface did not interfere with ice nucleation (Dymarska et al., 2006; Knopf and Lopez, 2009; Koop et al., 1998; Eastwood et al., 2009). The same procedure was used to examine homogeneous nucleation and the resulting nucleation rates were in good agreement with literature data, thus confirming that the surface did not initiate crystallisation (Murray et al., 2010a). Once enough droplets in the 10–40 µm diameter size range were deposited, a second cover slip with a spacer was placed over the first cover slip to encase the droplets in the N_2-filled space between the cover slips (i.e. the droplets were not in contact with the top cover slip). The amount of water vapour around the droplets was insufficient to significantly alter the concentration of the clay in the droplets as the cell was cooled, hence the dust concentration was fixed. This droplet-containing cell was then transferred to the cold stage where ice nucleation was measured.

3 Materials

Our approach was to measure the ice nucleating efficiency of well characterised dust samples which were predominantly composed of a single mineral. Natural dusts and Arizona Test Dust (ATD), the commonly employed proxy for natural dusts, are complex mixtures of minerals and, as is shown later in this paper, each mineral has distinct ice nucleating characteristics. Later in the paper we suggest that the wide range of freezing temperatures observed in immersion mode experiments (Marcolli et al., 2007; Vali, 2008) is a result of the wide range of minerals present in natural and test dusts. Furthermore, it is unclear if test dusts such as ATD are a suitable proxy for atmospheric mineral dusts. ATD is manufactured by milling and size grading, and is intended to be used to test the efficiency of air filters rather than as a proxy for atmospheric dust. The clay minerals examined in this study were kaolinite ($Al_4(OH)_8Si_4O_{10}$) and montmorillonite ($(Na,Ca)_{0.33}(Al,Mg)_2(Si_4O_{10})(OH)_2 \cdot nH_2O$), sourced from the Clay Mineral Society. This society make available well characterised clay mineral samples for research purposes which have not been acid washed or otherwise chemically treated (see Costanzo et al. (2001) and related special issue), unlike clays from chemical companies sometimes employed in other studies (Zuberi et al., 2002). We used Kaolinite KGa-1b and Montmorillonite SWy-2. Pertinent details are given in Table 1.

4 Results and discussion

4.1 Heterogeneous freezing temperatures

Using the optical microscope images we determined the fraction of droplets which froze [$f_{ice}(T) = n_{ice}(T)/n$, where n_{ice} is the number of frozen droplets and n is the total number of frozen or liquid droplets] as a function of temperature. Only droplets in the 10–40 µm size range were considered. Plots of f_{ice} for pure water and droplets contaminated with kaolinite and montmorillonite are shown in Fig. 1.

Pure water droplets were previously found to freeze homogeneously with a median freezing temperature (T_f) of 235.5±0.6 K for a cooling rate of 10 K min^{-1} using this apparatus (Murray et al., 2010a). The homogeneous nucleation rates derived from this data were in good agreement with literature data and showed that the surface did not catalyse ice formation. In contrast, droplets containing kaolinite froze between 235.5±0.6 K and 240.8±0.6 K (median freezing temperatures) depending on the concentration of kaolinite present; the more kaolinite the higher the freezing temperature. Droplets containing montmorillonite also froze well above the homogeneous limit with T_f=245.8±0.6 K, but we observed no dependence on the concentration of montmorillonite.

Pruppacher and Klett (1997) state that T_f of a population of droplets containing solid particles is a function of the droplet volume. We show that this is not the case for kaolinite. Instead T_f varies as a function of the surface area of kaolinite within the droplets (see Fig. 2). The surface area of kaolinite was varied by changing the concentration of kaolinite suspended in the droplets and holding the median droplet volume almost constant (it varied by less than a factor of two in a non-systematic manner, see Table 2). Pruppacher and Klett (1997) cite a number of articles which claim to show that T_f varied as a function of droplet volume. However, surface area of inclusions per droplet scales with droplet volume for a given inclusion concentration and therefore one would expect larger droplets to freeze at higher temperatures. We suggest that T_f is a function of the surface area of solid inclusions rather than the volume of the droplets. This distinction is critically important since it is assumed in modern parameterisations of immersion mode freezing (Diehl and Wurzler, 2004), which are used in global modelling studies (Lohmann and Diehl, 2006), that freezing is dependent on volume of the droplet rather than surface area of the inclusion.

Mason (1971) and Pruppacher and Klett (1997) review literature data for ice nucleation by a range of minerals. They quote ice nucleation temperature as high as 264 K for kaolinite and 257 K for montmorillonite. In these experiments powdered samples were injected into a chamber containing supercooled droplets and contact or deposition nucleation were most likely the dominant modes of ice nucleation. There are only a handful of literature reports of immersion mode ice nucleation for kaolinite and montmorillonite and this data is poorly quantified in terms of the amount of particulate material per droplet. Pitter and Pruppacher (1973) found that T_f for droplets contaminated with dust particles was 252 for montmorillonite and 248 K for kaolinite. These droplets were 325 µm in radius and the clay particle diameter varied from 0.1 to 30 µm with a mode diameter of between 1–2 µm. Freezing occurred over a range of ∼14 K in contrast to our experiments where freezing occurred within ∼5 K.

Hoffer (1961) reported median freezing temperatures for ∼50 µm radius droplets of 249 K and 240.7 K for an unknown quantity of montmorillonite and kaolinite, respectively. The result for kaolinite is within our concentration dependent spread of freezing temperatures, whereas Hoffer's median freezing temperature for montmorillonite is ∼3 K higher than our measurement. However, Hoffer noted that freezing occurred between 259.7 and 237.7 K, a spread of ∼22 K, whereas it occurred within ∼4 K in our experiments. The large spread in freezing temperatures led Hoffer to suggest that the montmorillonite they used might be impure. Hence, we suggest that our data is more representative of the ice nucleating properties of montmorillonite.

Freezing of millimetre sized droplets containing kaolinite was reported by Hama and Itoo (1953). They quote a median freezing temperature of 263 K, although their freezing range overlapped with that for distilled water which indicated their water was not free of ice nuclei. In general the literature data suggests that the larger the droplets, the high the freezing temperature. We suggest that the larger droplets simply contained a greater surface area of kaolinite and therefore froze at higher temperatures. Unfortunately, Hoffer (1961), Pitter and Pruppacher (1973) and Hama and Itoo (1953) did not report the concentration of mineral dusts in their droplets.

4.2 Rates of heterogeneous nucleation of ice on kaolinite

We determine temperature dependent nucleation rate constants for kaolinite (J_k) in units of nucleation events per unit area of clay per unit time from the data shown in

Fig. 1. The number of droplets which froze heterogeneously on kaolinite in a given time increment (Δt) can be expressed by

$$n_{\mathrm{het,k}} = n(1 - \exp(-J_{\mathrm{k}}(T)\sigma \Delta t)) \tag{1}$$

where n is the number of liquid droplets at the beginning of a time interval and σ is the surface area of particulate matter suspended in a droplet of median size (Marcolli et al., 2007). This equation is analogous to the equations used to describe homogeneous nucleation (Murray et al., 2010a), but droplet volume is replaced by surface area of solid within a droplet and J_{hom} (cm^{-3} s^{-1}) is replaced by J_{k} (cm^{-2} s^{-1}). We are therefore assuming that heterogeneous nucleation on kaolinite is a stochastic process, an assumption which is supported later in the paper. Pruppacher and Klett (1997) state that heterogeneous freezing is related to droplet volume, but it was shown above that freezing is actually determined by the surface area of kaolinite inclusions, hence the units of J_{k}. Using Eq. (1), we produce an average nucleation rate within each time interval and therefore establish the temperature (T) dependence of J_{k}.

The surface area of mineral dust in a droplet of median size was calculated from the concentration of mineral dust in the droplets in combination with the specific surface area of the clay mineral. The specific surface areas of kaolinite and montmorillonite samples have been reported in the literature and are summarised in Table 1. We used the average values in our calculations. Gas adsorption techniques are in agreement with atomic force microscopy measurements of surface area for kaolinite (Bickmore et al., 2002). The surface area of kaolinite per median droplet in the experiments was varied from 2.6×10^{-8} to 3.7×10^{-6} cm^{-2}, which corresponds to equivalent spherical kaolinite particles with radius between 0.45 and 5.5 µm (see Table 2).

The median volume of the droplets for each experiment is presented in Table 2 together with the mean surface area of clay particles per droplet. In order to calculate temperature dependent nucleation rates we chose a Δt of 3 s. A shorter time interval would have the advantage of improving the temperature resolution of J_{k}, but each time bin would have less freezing events which would increase the statistical error. J_{k} was only reported for time intervals in which there was at least one freezing event within that time increment as well as in the following or preceding time increment. Hence, sporadic freezing events at the beginning and end of the fraction frozen curves (Fig. 1) were not included in the analysis. In addition, we only determined values of J_k for data above 236.1 K since homogeneous nucleation becomes important below this temperature.

The resulting nucleation rates for kaolinite are shown as a function of temperature in Fig. 3. The temperature dependent values of J_k for all the experiments fall on a single line within experimental uncertainty. This plot clearly shows, for the first time, that the rate at which kaolinite nucleates ice when immersed in droplets scales with the surface area of kaolinite present in the droplets.

4.3 Rates of heterogeneous nucleation of ice on montmorillonite

The fraction frozen curves in Fig. 1 for droplets contaminated with varying amounts of montmorillonite clearly show that the freezing threshold is independent of the amount of montmorillonite. Analysis of this data therefore requires a different approach to that employed for kaolinite in which the rate of freezing was related to the surface area.

It is unclear to us at this time why ice nucleation by montmorillonite does not scale with surface area. Heterogeneous ice nucleation is a process in which molecules adsorb on a surface and is therefore analogous with heterogeneous catalysis. Catalysis may become saturated at high reactant concentrations, but one would still expect the rate of reaction (or nucleation) to increase as the surface area of catalyst increases. Montmorillonite's unusual ice nucleating properties may be related to its very flexible structure. Montmorillonite is known to be an expansive clay that can accept large quantities of water between its silicate layers (Deer et al., 1966). This property may influence its ability to nucleate ice. More work is needed to fully understand ice nucleation by montmorillonite.

We define a new heterogeneous nucleation rate constant, J'_m, with units s^{-1}. $J'_m(T)$ has been determined from the fraction frozen data using the following equation:

$$n_{\mathrm{het},m} = n(1 - \exp(-J'_m(T)\Delta t)) \tag{2}$$

The resulting values of J'_m are shown in Fig. 4 and they clearly fall on a single line, confirming the independence of rate on surface area. J'_m provides a means of describing ice nucleation by montmorillonite at least in the range of surface areas and temperatures experimentally probed here.

4.4 Fitting kaolinite ice nucleation rates to heterogeneous nucleation theory

In the absence of a solid surface, the energy barrier to the nucleation of an ice crystal from pure water (homogeneous nucleation) can be expressed by

$$\Delta G^* = \frac{16\pi\gamma^3 v^2}{3(kT\ln S)^2} \tag{3}$$

where γ is the interfacial energy between ice and supercooled water, v is the molecular volume of water in ice, k is the Boltzmann constant and S is the saturation ratio with respect to ice. S is defined as $P_\mathrm{l}/P_\mathrm{ice}$ (Murray et al., 2010a), where P_l is the equilibrium vapour pressure over a flat liquid water surface and P_ice is the equilibrium vapour pressure over a flat ice surface. The temperature dependent rate of heterogeneous nucleation (cm^{-2} s^{-1}) can then be described by an equation in an Arrhenius form:

$$J(T) = A_\mathrm{het}\exp\left(-\frac{\Delta G^*\phi}{kT}\right) \tag{4}$$

where A_het is a pre-exponential factor in units of cm^{-2} s^{-1}. In the case of heterogeneous nucleation, the presence of a solid surface reduces the height of the energy barrier relative to homogeneous nucleation by a factor ϕ which can be expressed in terms of an ice nucleating efficiency parameter, m:

$$\phi = \frac{(2+m)(1-m)^2}{4} \tag{5}$$

The parameter m is equal to $\cos\theta$, where θ is the contact angle of a spherical ice nucleus in contact with a flat surface. While the concept of a spherical ice cluster on a flat surface is a useful concept in terms of deriving simple equations, its physical meaning is unclear. Hence we report values of m which can be regarded as a quantitative, semi-empirical, measure of a substance's ability to nucleate ice. A value of m=1 would correspond to a perfect ice nucleus (ϕ=0), whereas a value of −1 would indicate that the surface did not nucleate ice (ϕ=1).

Combining Eqs. (3), (4), and (5) we see that the heterogeneous nucleation rate can be expressed as (Mullin, 2001; Pant et al., 2006; Parsons et al., 2006):

$$\ln J = \ln A_{\mathrm{het}} - \frac{16\pi\gamma^3 v^2}{3k^3T^3(\ln S)^2}\frac{(2+m)(1-m)^2}{4} \tag{6}$$

Hence, over a narrow range in temperatures a plot of ln J versus $T^{-3}(\ln S)^{-2}$ yields a linear plot with slope

$$M = -\frac{16\pi\gamma^3 v^2}{3k^3}\frac{(2+m)(1-m)^2}{4} \tag{7}$$

thus providing a means of determining m if γ is known, without the need to estimate A_{het}.

There are two crystalline phases of ice that can form at atmospheric pressures and therefore there are two possible solutions to this equation. The stable phase of ice has a hexagonal crystal structure (ice $\mathrm{I_h}$), but there is also a metastable phase with a cubic crystal structure (ice $\mathrm{I_c}$). Diffraction work has shown that ice $\mathrm{I_c}$ is the phase to nucleate and crystallise from pure water droplets when they freeze homogeneously (Huang and

Bartell, 1995; Murray and Bertram, 2006, 2007; Murray et al., 2005) and also when solution droplets freeze homogeneously (Murray, 2008; Murray and Bertram, 2008; Murray et al., 2005). Unfortunately, diffraction studies of droplets freezing heterogeneously have not been done, so it is not known which phase nucleates and initially crystallises.

Ostwald's rule of stages states that a metastable phase should nucleate in preference to a more stable phase (Mullin, 2001). Indeed, the interfacial energy of the ice $\mathrm{I_c}$ – supercooled water interface is smaller than that of ice $\mathrm{I_h}$; this favours the nucleation of ice $\mathrm{I_c}$ in the case of homogeneous nucleation. However, in the case of heterogeneous nucleation by clay particles we also have to consider the clay-ice interfacial energy, which might favour one or other of the phases depending on how well the respective cluster fits to the structure of the solid surface. In addition, the value of S is larger for ice $\mathrm{I_h}$ than ice $\mathrm{I_c}$ since the latter is metastable. Hence, the thermodynamic potential is greater for the more stable phase and above a certain temperature the rate at which ice $\mathrm{I_h}$ nucleates will exceed that at which ice $\mathrm{I_c}$ nucleates. Since we can not categorically state which phase nucleates first we analyse our data for both phases in turn. This involves using the appropriate values of γ and S for each phase.

4.4.1 Assuming hexagonal ice nucleates

We take a value of 33±3 mJ m^{-2} for the supercooled water-ice $\mathrm{I_h}$ interfacial energy (γ_{Ih}) (Hobbs, 1974). The saturation ratio with respect to ice I_h, S_{Ih}, is equal to $P_{\mathrm{liq}}/P_{\mathrm{Ih}}$, where P_{Ih} is the vapour pressure over a flat ice $\mathrm{I_h}$ surface. Values of P_{liq} and P_{Ih} are taken from the review of Murphy and Koop (2005). The molecular volume is identical within experimental uncertainty for both ice phases (Dowell and Rinfret, 1960), and we use the parameterisation from Murray and Jensen (Murray and Jensen, 2010).

The resulting plot of ln J_{k} vs. $T^{-3}(\ln S_{\mathrm{Ih}})^{-2}$ is shown in Fig. 5. These plots yield m_{Ih} for kaolinite of 0.56±0.01, which corresponds to contact angles of 55.6±1.0° and ϕ of 0.121±0.007.

4.4.2 Assuming cubic ice nucleates

The supercooled water-ice I_c interfacial energy (γ_{Ic}) was recently determined through homogeneous freezing experiments to be 20.8±1.2 mJ m^{-2} (Murray et al., 2010a) at 235.8 K and has a weak temperature dependence. The homogeneous freezing experiments were performed using the same equipment and similar procedures to those employed in the present study. The saturation ratio with respect to ice I_c, S_{Ic}, is equal to P_{liq}/P_{Ic}, where P_{Ic} is the vapour pressure over a flat ice I_c surface. The difference in free energy between the two phases ($\Delta G_{h\rightarrow c}$) was recently determined at 180–190 K from relative vapour pressure measurements to be 155±30 J mol^{-1} (Shilling et al., 2006). If we assume $\Delta G_{h\rightarrow c}$ is temperature independent, we can approximate the temperature dependence of P_{Ic} as $P_{Ih}\exp(\Delta G_{h\rightarrow c}/RT)$ (Murphy, 2003; Murphy and Koop, 2005; Murray et al., 2010a). The plot in Fig. 5 yields m_{Ic} for kaolinite of 0.41±0.02, which corresponds to contact angles of 65.8±1.3° and ϕ of 0.210±0.013.

4.5 Parameterisations to describe ice nucleation in the immersion mode

In this section we suggest a way of parameterising immersion mode ice nucleation. The parameterisation takes into account time (cooling rate) and the surface area of kaolinite. This represents a significant improvement on parameterisations used in the past which neglect cooling rate and particle surface area effects (Diehl et al., 2006; Hoose et al., 2008; Lohmann and Diehl, 2006).

Let us consider a population of water droplets containing mineral dust particles. Ice can either nucleate on the mineral dust inclusion or in the bulk liquid. The number of droplets which freeze in a time interval will be equal to the sum of the droplets which freeze homogeneously and those which freeze heterogeneously.

$$dn_{ice} = dn_{hom} + dn_{het} \tag{8}$$

Expressions for dn_{hom}, $dn_{het,k}$ (dn_{het} for kaolinite) and $dn_{het,m}$ (dn_{het} for montmorillonite) can be written

$$dn_{\mathrm{hom}} = n_{\mathrm{liq}}(1-\exp(-J_{\mathrm{hom}}(T)V\,dt)) \tag{9}$$

$$dn_{\mathrm{het,k}} = n_{\mathrm{liq,k}}(1-\exp(-J_{\mathrm{k}}(T)\sigma\,dt)) \tag{10}$$

$$dn_{\mathrm{het},m} = n_{\mathrm{liq},m}(1-\exp(-J'_{m}(T)\,dt)) \tag{11}$$

where n_{liq} is the number of water droplets of volume V at the beginning of a time increment, $n_{\mathrm{liq,k}}$ is the number of liquid water droplets which contain kaolinite with surface area σ and $n_{\mathrm{liq},m}$ is the number of droplets which contain montmorillonite. Note that n_{liq} is the total number of liquid droplets including those containing particles which may serve as ice nuclei which are still liquid (i.e. there is competition between homogeneous and heterogeneous nucleation within individual droplets). The surface area of montmorillonite is not defined since $J_{m'}$ is in units of s^{-1}.

The temperature dependent nucleation rates based on our data are given by (J_{hom} is taken from Murray et al., 2010a)

$$J_{\mathrm{hom}}(T) = \exp(-2.92T + 706.5)\ (234.9-236.7\,\mathrm{K}) \tag{12}$$

$$J_{\mathrm{k}}(T) = \exp(-0.8484T + 214.34)\ (236.1-242.3\,\mathrm{K}) \tag{13}$$

$$J'_{m}(T) = \exp(-0.9897T + 241.0)\ (244.3-248.1\,\mathrm{K}) \tag{14}$$

These exponential parameterisation were derived from fits to the data which were recorded over the temperature ranges given in brackets. Over the temperature range of interest for mixed phase clouds these parameterisations provide a reasonable approximation of the respective nucleation rates.

To show that these equations (Eqs. 8–14) are self consistent with our experimental data we have plotted the parameterised and experimental $f_{\mathrm{ice}}(T)$ for kaolinite in Fig. 6. $f_{\mathrm{ice}}(T)$ is defined is Sect. 4.1 as the ratio of $n_{\mathrm{ice}}(T)$ to n. The total number of frozen droplets ($n_{\mathrm{ice}}(T)$) is the integral number of droplets which froze on cooling to T at a defined cooling rate. We solve this integral by calculating dn_{ice} for appropriately small increments in temperature and summing the number of droplets which froze at each increment to determine $n_{ice}(T)$. The resulting values of $f_{ice}(T)$ are in good agreement with our data, as expected (see Fig. 6).

Inspection of $f_{ice}(T)$ for 0.005 wt% kaolinite in Fig. 6 reveals that heterogeneous nucleation on the kaolinite particles competes with homogeneous nucleation. The dotted line is $f_{ice}(T)$ for heterogeneous nucleation on kaolinite only and this clearly under predicts the experimentally determined f_{ice} below 236 K. We have also included f_{ice} for homogeneous freezing (dashed line). The rate at which droplets freeze homogeneously exceeds that at which they freeze heterogeneously at 235.7 K (for these specific conditions) and inclusion of both homogenous and heterogeneous nucleation yield a good fit to the data (solid line). Freezing of droplets with a greater concentration of kaolinite (0.1 wt% and 1.0 wt%) is dominated by heterogeneous nucleation.

The competition between homogeneous nucleation and heterogeneous nucleation within droplets contaminated with mineral dust particles can be understood with the help of Fig. 7. In this figure we have plotted the average time required for 50% of a monodispersed population of droplets to freeze (t_{50}) as a function of temperature. We have plotted three curves, the first for 20 µm diameter pure water droplets which freeze homogeneously, the second for droplets of unspecified volume each contaminated with a spherical kaolinite particle of 1 µm diameter and the third for droplets contaminated with montmorillonite particles.

The time required for homogeneous nucleation varies much more steeply with temperature than heterogeneous nucleation on either of the mineral dusts. This is important because homogeneous nucleation is therefore much better approximated by a threshold freezing temperature than heterogeneous nucleation. A step function for freezing on clay minerals is inappropriate since nucleation has significant time dependence. The difference in temperature dependence also means that the line for heterogeneous nucleation on kaolinite intersects the line for homogeneous nucleation at 236.6 K. Below this temperature the rate of homogeneous nucleation in a 20 µm droplet becomes more rapid than the rate of heterogeneous nucleation on the 1 µm mineral dust inclusion. This threshold will obviously depend on the volume of the droplet and size of the kaolinite particle. In larger droplets homogeneous nucleation will become more important at higher temperatures and for larger inclusions heterogeneous nucleation will become more important at higher temperatures.

In Fig. 8 we illustrate the dependence of f_{ice} on cooling rate based on the parameterisations outlined in Eqs. (8) to (14). These calculations are for spherical kaolinite particles of 1 µm diameter immersed in droplets of 20 µm diameter. The size of the water droplet is only significant for the lowest temperatures (fastest cooling rates for kaolinite) where homogeneous nucleation competes with heterogeneous nucleation. The size of montmorillonite is not defined since it displays no surface area dependence for micron-sized particles. On changing the cooling rate from 10 to 0.01 K min^{-1} the freezing curves shifts to higher temperatures by 7 K for montmorillonite and 8 K for kaolinite. This is in contrast to a change in just 2 K for homogeneous nucleation over a similar range of cooling rates.

In Fig. 7, we have also plotted f_{ice} based on the parameterisation of Diehl and Wurzler (2004) for both kaolinite and montmorillonite immersed in 20 µm diameter droplets. Diehl and Wurzler present a cooling rate and surface area independent parameterisation in which the rate of droplet freezing is a function of droplet volume rather than surface area of clay particle. Our parameterisation shows that droplets contaminated by montmorillonite will freeze at significantly higher temperatures than indicated by the parameterisation of Diehl and Wurzler. In addition, it is also clear that it is important to include the cooling rate dependence in order to better describe ice nucleation by mineral dusts.

5 Summary and conclusions

We present the first quantitative measurements of the rate at which kaolinite and montmorillonite nucleate ice in the immersion mode. For an experimental cooling rate of

10 K min^{-1}, the median nucleation temperature increased from close to the homogeneous nucleation limit (236 K) to 240.8±0.6 K as the kaolinite concentration was increased from 0.005 wt% to 1 wt%. In contrast, ice always nucleated at a median temperature of 245.8±0.6 K when water droplets were contaminated with varying concentrations of montmorillonite. In these experiments a population of droplets containing a similar amount of mineral dust froze within a narrow range of temperatures (~5 K), indicating that heterogeneous nucleation occurred at some defined rate in a stochastic manner. This is in contrast to previous work in which droplets contaminated with Arizona Test Dust (ATD) froze over a range of 20 K (Marcolli et al., 2007). We suggest that this spread in nucleation temperatures is due to the fact that ATD is made up of a range of minerals, each with its own ice nucleating properties. This highlights the need to examine the ice nucleating properties of individual minerals in addition to complex mixtures of minerals such as natural desert dusts.

We show that the rate of nucleation of ice by kaolinite in the immersion mode is a function of the surface area of clay within each droplet. This is in contrast to parameterisations used in models which assume the freezing rate is a function of the droplet volume (Bigg, 1953; Diehl and Wurzler, 2004; Pruppacher and Klett, 1997; Vali, 1994). We went on to show that immersion mode ice nucleation by kaolinite can be described by a single contact angle which is insensitive to temperature (at least in the range of temperatures probed here). This suggests that one kaolinite particle has very similar or identical ice nucleating properties to another kaolinite particle and kaolinite particles of the same size have the same probability of nucleating ice under a given set of conditions. We now need to test if kaolinite from other sources has the same ice nucleating properties as the sample used here.

In contrast to ice nucleation on kaolinite, nucleation rates of ice on montmorillonite do not scale with the amount of montmorillonite present in droplets. The stochastic and singular models of heterogeneous ice nucleation are commonly referred to in the literature and can be used to rationalise laboratory observations (Martin, 2000; Pruppacher and Klett, 1997). Homogeneous nucleation is a stochastic process and in the stochastic model of heterogeneous nucleation, critical cluster formation is similarly time dependent. Pruppacher and Klett (1997) argue that the probability of heterogeneous nucleation in the stochastic model is a function of droplet volume, but we show that for kaolinite it is a function of surface area of clay inclusions. For montmorillonite the freezing temperature does not appear to scale with surface area, hence nucleation on montmorillonite is inconsistent with the stochastic model. In the singular model individual particles within a droplet nucleate ice at some well defined and reproducible threshold temperature and there is no dependence on time (or cooling rate). The shape of the fraction frozen curves in Fig. 1 which are used to calculate a time dependent nucleation rate constant in Fig. 4 strongly suggest that the nucleation probability is time dependent, with an increasing rate of freezing as the temperature falls. Hence, nucleation on montmorillonite does not fit with either the stochastic or the singular model. Further work needs to be done to explain montmorillonite's unexpected behaviour and should include a detailed study of dependence of nucleation on time, surface area of montmorillonite (for smaller surface areas) and droplet volume.

Acknowledgements. We thank Zhiqiang Cui for helpful discussions and Trevor Ingham for help with automation of the data logging. We acknowledge the Natural Environment Research Council (NE/D009308/1 and NE/H001050/1) and the European Research Council (240449 – ICE) for financial support. TWW thanks the Charles Brotherton trust for a Studentship and the Aerosol Society for other financial support.

References

Bereznitski, Y., Jaroniec, M., and Maurice, P.: Adsorption characterization of two clay minerals society standard kaolinites, J. Coll. Interface Sci., 205, 528–530, 1998.
Bickmore, B. R., Nagy, K. L., Sandlin, P. E., and Crater, T. S.: Quantifying surface areas of clays by atomic force microscopy, Amer. Mineralogist, 87, 780–783, 2002.
Bigg, E. K.: The supercooling of water, Proc. Phys. Soc., 66, 688–694, 1953.
Costanzo, P. M.: Baseline studies of the clay minerals society source clays: Introduction, Clays and Clay Minerals, 49, 372–373, 2001.

Deer, W. A., Howie, R. A., and Zussman, J.: An introduction to the rock forming minerals, Longman, London, 1966.

DeMott, P. J.: Laboratory studies of cirrus cloud processes, in: Cirrus, edited by: Lynch, D. K., Sassen, K., Starr, D. C., and Stephens, G., Oxford University Press, Oxford, 102–135, 2002.

DeMott, P. J., Cziczo, D. J., Prenni, A. J., Murphy, D. M., Kreidenweis, S. M., Thomson, D. S., Borys, R., and Rogers, D. C.: Measurements of the concentration and composition of nuclei for cirrus formation, Proc. Natl. Acad. Sci. USA, 100, 14655–14660, 2003a.

DeMott, P. J., Sassen, K., Poellot, M. R., Baumgardner, D., Rogers, D. C., Brooks, S. D., Prenni, A. J., and Kreidenweis, S. M.: African dust aerosols as atmospheric ice nuclei, Geophys. Res. Lett., 30, 1732, doi:10.1029/2003GL017410, 2003b.

Denman, K. L., Brasseur, G., Chidthaisong, A., Ciais, P., Cox, P. M., Dickinson, R. E., Hauglustaine, D., Heinze, C., Holland, E., Jacob, D., Lohmann, U., Ramachandran, S., da Silva Dias, P. L., Wofsy, S. C., and Zhang, X.: Couplings between changes in the climate system and biogeochemistry, in: Climate change 2007: The physical science basis. Contribution of working group i to the fourth assessment report of the intergovernmental panel on climate change, edited by: Solomon, S., D., Qin, M., Manning, Z., Chen, M., Marquis, K. B., Averyt, M. T., and Miller, H. L., Cambridge University Press, Cambridge, 2007.

Diehl, K. and Wurzler, S.: Heterogeneous drop freezing in the immersion mode: Model calculations considering soluble and insoluble particles in the drops, J. Atmos. Sci., 61, 2063–2072, 2004.

Diehl, K., Simmel, M., and Wurzler, S.: Numerical sensitivity studies on the impact of aerosol properties and drop freezing modes on the glaciation, microphysics, and dynamics of clouds, J. Geophys. Res., 111, D07202, doi:10.1029/2005JD005884, 2006.

Dogan, A. U., Dogan, M., Onal, M., Sarikaya, Y., Aburub, A., and Wurster, D. E.: Baseline studies of the clay minerals society source clays: Specific surface area by the brunauer emmett teller (bet) method, Clay and Clay Minerals, 54, 62–66, 2006.

Dowell, L. G. and Rinfret, A. P.: Low-temperature forms of ice as studied by x-ray diffraction, Nature, 188, 1144–1148, 1960.

Dymarska, M., Murray, B. J., Sun, L. M., Eastwood, M. L., Knopf, D. A., and Bertram, A. K.: Deposition ice nucleation on soot at temperatures relevant for the lower troposphere, J. Geophys. Res., 111, D04204, doi:10.1029/2005JD006627, 2006.

Eastwood, M. L., Cremel, S., Wheeler, M., Murray, B. J., Girard, E., and Bertram, A. K.: The effects of sulfuric acid and ammonium sulfate coatings on the ice nucleation properties of kaolinite particles, Geophys. Res. Lett., 36, L02811 doi:02810.01029/02008GL035997, 2009.

Foster, A. L., Brown Jr, G. E., and Parks, G. A.: X-ray absorption fine-structure spectroscopy of photocatalyzed, heterogeneous as(iii) oxidation on kaolin and anatase, Environ. Sci. Technol., 32, 1444–1452, 1998.

Glaccum, R. A. and Prospero, J. M.: Saharan aerosol over the tropical North Atlantic – mineralogy, Mar. Geol., 37, 295–321, 1980.

Gregg, S. L. and Sing, K. S. W.: Adsorption surface area and porosity, Academic Press, London, 1982.

Hama, K. and Itoo, K.: Freezing of supercooled water droplets (ii), Pap. Met. Geophys., 7, 99–106, 1953.

Hobbs, P.: Ice physics, Oxford University Press, London, 1974.

Hoffer, T. E.: A laboratory investigation of droplet freezing, J. Meteorol., 18, 766–778, 1961.

Hoose, C., Lohmann, U., Erdin, R., and Tegen, I.: The global influence of dust mineralogical composition on heterogeneous ice nucleation in mixed-phase clouds, Env. Res. Lett., 3, 025003, doi:10.1088/1748-9326/3/2/025003, 2008.

Huang, J. F. and Bartell, L. S.: Kinetics of homogeneous nucleation in the freezing of large water clusters, J. Phys. Chem., 99, 3924–3931, 1995.

Jaynes, W. F., Zartman, R. E., Green, C. J., San Francisco, M. J., and Zak, J. C.: Castor toxin adsorption to clay minerals, Clay and Clay Minerals, 53, 268–277, 2005.

Kandler, K., Benker, N., Bundke, U., Cuevas, E., Ebert, M., Knippertz, P., Rodriguez, S., Schutz, L., and Weinbruch, S.: Chemical composition and complex refractive index of saharan mineral dust at izana, tenerife (spain) derived by electron microscopy, Atmos. Environ., 41, 8058–8074, 2007.

Knopf, D. A. and Lopez, M. D.: Homogeneous ice freezing temperatures and ice nucleation rates of aqueous ammonium sulfate and aqueous levoglucasan particles for relevant atmospheric conditions, Phys. Chem. Chem. Phys., 11, 8056–8068, 2009.

Koop, T., Ng, H. P., Molina, L. T., and Molina, M. J.: A new optical technique to study aerosol phase transitions: The nucleation of ice from h2so4 aerosols, J. Phys. Chem. A, 102, 8924–8931, 1998.

Koren, I., Kaufman, Y. J., Washington, R., Todd, M. C., Rudich, Y., Martins, J. V., and Rosenfeld, D.: The bodele depression: A single spot in the sahara that provides most of the mineral dust to the amazon forest, Environ. Res. Lett., 1, 014005, doi:014010.011088/011748-019326/014001/014001/014005, 2006.

Lohmann, U. and Feichter, J.: Global indirect aerosol effects: a review, Atmos. Chem. Phys., 5, 715–737, 2005,
http://www.atmos-chem-phys.net/5/715/2005/.

Lohmann, U. and Diehl, K.: Sensitivity studies of the importance of dust ice nuclei for the indirect aerosol effect on stratiform mixed-phase clouds, J. Atmos. Sci., 63, 968–981, 2006.

Mahowald, N. M. and Kiehl, L. M.: Mineral aerosol and cloud interactions, Geophys. Res. Lett., 30, 1475, doi:10.1029/2002GL016762, 2003.

Marcolli, C., Gedamke, S., Peter, T., and Zobrist, B.: Efficiency of immersion mode ice nucleation on surrogates of mineral dust, Atmos. Chem. Phys., 7, 5081–5091, 2007,
http://www.atmos-chem-phys.net/7/5081/2007/.

Martin, S.: Phase transitions of aqueous atmospheric particles, Chem. Rev., 100, 3403–3453, 2000.

Mason, B. J.: The physics of clouds, Clarendon Press, Oxford, 1971.

Mertes, S., Verheggen, B., Walter, S., Connolly, P., Ebert, M., Schneider, J., Bower, K. N., Cozic, J., Weinbruch, S., Baltensperger, U., and Weingartner, E.: Counterflow virtual impact or based collection of small ice particles in mixed-phase clouds for the physico-chemical characterization of tropospheric ice nuclei: Sampler description and first case study, Aerosol Sci. Technol., 41, 848–864, 2007.

Mullin, J. W.: Crystallization, Forth ed., Elsevier Butterworth-Heinemann, Oxford, 2001.

Murphy, D. M.: Dehydration in cold clouds is enhanced by a transition from cubic to hexagonal ice, Geophys. Res. Lett., 30, 2230, doi:2210.1029/2003GL018566, 2003.

Murphy, D. M. and Koop, T.: Review of the vapour pressures of ice and supercooled water for atmospheric applications, Q. J. Roy. Meteorol. Soc., 131, 1539–1565, 2005.

Murray, B. J., Knopf, D. A., and Bertram, A. K.: The formation of cubic ice under conditions relevant to earth's atmosphere, Nature, 434, 202–205, 2005.

Murray, B. J. and Bertram, A. K.: Formation and stability of cubic ice in water droplets, Phys. Chem. Chem. Phys., 8, 186–192, 2006.

Murray, B. J. and Bertram, A. K.: Laboratory studies of the formation of cubic ice in aqueous droplets, in: Physics and chemistry of ice, edited by: Kuhs, W. F., The Royal Society of Chemistry, Cambridge, 417–426, 2007.

Murray, B. J.: Enhanced formation of cubic ice in aqueous organic acid droplets, Env. Res. Lett., 3, 025008, doi:025010.021088/021748-029326/025003/025002/025008, 2008.

Murray, B. J. and Bertram, A. K.: Inhibition of solute crystallisation in aqueous h+ – nh4+ –

so42- – h2o droplets Phys. Chem. Chem. Phys., 10, 3287–3301, doi:3210.1039/B802216J, 2008.

Murray, B. J., Broadley, S., Wilson, T. W., Bull, S., and Wills, R.: Kinetics of the homogeneous freezing of water, Phys. Chem. Chem. Phys., submitted, 2010a.

Murray, B. J. and Jensen, E. J.: Homogeneous nucleation of amorphous solid water particles in the upper mesosphere, J. Atmos. Solar-Terr. Phys., 72, 51–61, doi:10.1016/j.jastp.2009.1010.1007, 2010.

Murray, B. J., Wilson, T. W., Dobbie, S., Cui, Z., Al-Jumur, S. M. R. K., Möhler, O., Schnaiter, M., Wagner, R., Benz, S., Niemand, M., Saathoff, H., Ebert, V., Wagner, S., and Kärcher, B.: Heterogeneous nucleation of ice particles on glassy aerosols under cirrus conditions, Nature Geosci., 3, 233–237, doi:10.1038/NGEO1817, 2010b.

Pant, A., Parsons, M. T., and Bertram, A. K.: Crystallization of aqueous ammonium sulfate particles internally mixed with soot and kaolinite: Crystallization relative humidities and nucleation rates, J. Phys. Chem. A, 110, 8701–8709, 2006.

Parsons, M. T., Riffell, J. L., and Bertram, A. K.: Crystallization of aqueous inorganic-malonic acid particles: Nucleation rates, dependence on size, and dependence on the ammonium-to-sulfate, J. Phys. Chem. A, 110, 8108–8115, 2006.

Pitter, R. L. and Pruppacher, H. R.: A wind tunnel investigation of freezing of small water drops falling at terminal velocity in air, Q. J. Roy. Meteorol. Soc., 99, 540–550, 1973.

Pratt, K. A., DeMott, P. J., French, J. R., Wang, Z., Westphal, D. L., Heymsfield, A. J., Twohy, C. H., Prenni, A. J., and Prather, K. A.: In situ detection of biological particles in cloud ice-crystals, Nature Geoscience, 2, 398–401, doi:310.1038/NGEO1521, 2009.

Prenni, A. J., Petters, M. D., Kreidenweis, S. M., Heald, C. L., Martin, S. T., Artaxo, P., Garland, R. M., Wollny, A. G., and Pöschl, U.: Relative roles of biogenic emissions and saharan dust as ice nuclei in the amazon basin, Nature Geosci., 2, 402–405, doi:410.1038/NGEO1517, 2009.

Pruppacher, H. R. and Klett, J. D.: Microphysics of clouds and precipitation, Kluwer, Dordrecht, 1997.

Richardson, M. S., DeMott, P. J., Kreidenweis, S. M., Cziczo, D. J., Dunlea, E. J., Jimenez, J. L., Thomson, D. S., Ashbaugh, L. L., Borys, R. D., Westphal, D. L., Casuccio, G. S., and Lersch, T. L.: Measurements of heterogeneous ice nuclei in the western united states in springtime and their relation to aerosol characteristics, J. Geophys. Res., 112, D02209, doi:10.1029/2006JD007500, 2007.

Sassen, K.: Dusty ice clouds over alaska, Nature, 434, 456–456, 2005.

Shilling, J. E., Tolbert, M. A., Toon, O. B., Jensen, E. J., Murray, B. J., and Bertram, A. K.: Measurements of the vapor pressure of cubic ice and their implications for atmospheric ice clouds, Geophys. Res. Lett., 33, L17801, doi:17810.11029/12006gl026671, 2006.

Thompson, H. A., Parks, G. A., and Brown Jr., G. E.: Dynamic interactions of dissolution, surface adsorption,, and precipitation in an ageing cobalt(ii)-clay-water system, Geochim. Cosmochim. Acta, 63, 1767–1779, 1999.

Usher, C. R., Michel, A. E., and Grassian, V. H.: Reactions on mineral dust, Chem. Rev., 103, 4883–4939, 2003.

Vali, G.: Nucleation terminology, J. Aerosol Sci., 16, 575–576, 1985.

Vali, G.: Freezing rate due to heterogeneous nucleation, J. Atmos. Sci., 51, 1843–1856, 1994.

Vali, G.: Repeatability and randomness in heterogeneous freezing nucleation, Atmos. Chem. Phys., 8, 5017–5031, 2008, http://www.atmos-chem-phys.net/8/5017/2008/.

Zhang, X. Y., Arimoto, R., and An, Z. S.: Dust emission from chinese desert sources linked to variations in atmospheric circulation, J. Geophys. Res., 102, 28041–28041, 1997.

Zuberi, B., Bertram, A. K., Cassa, C. A., Molina, L. T., and Molina, M. J.: Heterogeneous nucleation of ice in (nh4)2so4-h2o particles with mineral dust immersions, Geophys. Res. Lett., 29, 1504, doi:10.1029/2001GL014289, 2002.

Table 1. Properties of "as shipped" clay minerals used in this study.

Mineral	Purity	Major impurities	Surface area/$m^2 g^{-1}$
Kaolinite (KGa-2)	96%	Anatase, crandallite, mica, illite.	13.1 (N_2 BET[a]) (Dogan et al., 2006)
			11.3 (AFM[b]) (Bickmore et al., 2002)
			12.5 (N_2 BET[a]) (Bereznitski et al., 1998)
			11 (N_2 BET[a]) (Jaynes et al., 2005)
			12 (EGME[c]) (Jaynes et al., 2005)
			11.4 (N_2 BET[a]) (Foster et al., 1998)
			11.4 (N_2 BET[a]) (Thompson et al., 1999)
			Average = 11.8±0.8
Montmorillonite SWy-2	75%	Quartz, feldspar, gypsum.	22.7 (N_2 BET[a]) (Dogan et al., 2006)
			27 (N_2 BET[a]) (Jaynes et al., 2005)
			24 (N_2 BET[a]) (Foster et al., 1998)
			Average = 25±2

[a] BET = Brauner Emmit and Teller gas adsorption technique (Gregg and Sing, 1982).
[b] AFM = Atomic force microscopy.
[c] EGME = Ethylene Glycol monoethyl ether adsorption.

Table 2. Parameters for each experiment used in the calculation of nucleation rates.

Clay mineral	Concentration/ wt%	Median volume[a]/ 10^{-9} cm^3	Median volume diameter[b]/µm	Surface area of clay per droplet/cm^{b}	Spherical equivalent radius of clay[c]/µm
Kaolinite	0.005	4.28	20.3	2.59×10^{-8}	0.45
	0.05	5.69	22.2	3.36×10^{-7}	1.63
	0.05	5.22	21.5	3.09×10^{-7}	1.58
	0.1	4.54	20.6	5.37×10^{-7}	2.07
	1.0	3.25	18.4	3.84×10^{-6}	5.53
	1.0	3.15	18.2	3.72×10^{-6}	5.44
Montmorillonite	0.05	4.57	20.6	5.62×10^{-7}	2.11
	0.05	4.23	20.1	5.19×10^{-7}	2.03
	0.10	4.84	21.0	1.19×10^{-6}	3.08
	1.0	4.71	20.8	1.16×10^{-5}	9.60
	1.0	5.00	21.2	1.23×10^{-5}	9.89

[a] The median droplet volume taking into account the contact angle of the droplets with the surface.

[b] This is the equivalent diameter of spheres determined from the volume in the preceding column.

[c] This is the radius of a spherical clay particle which would have the same surface area as the collection of smaller particles in a median droplet sized in our experiments.

a) Kaolinite

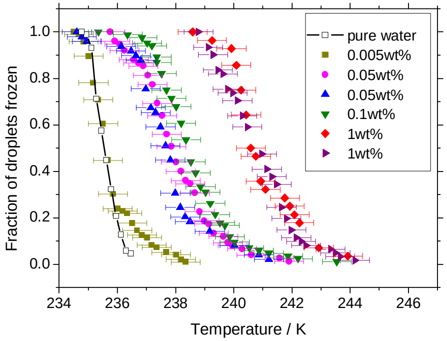

b) Montmorillonite

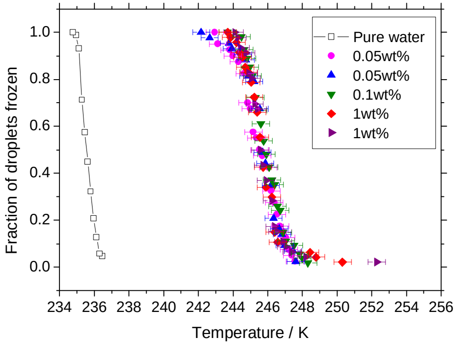

Fig. 1. Fraction of droplets frozen as a function of temperature as water droplets containing known concentrations of mineral dust are cooled down at 10 K min^{-1}. The data for pure water (homogeneous) is from Murray et al. (2010a).

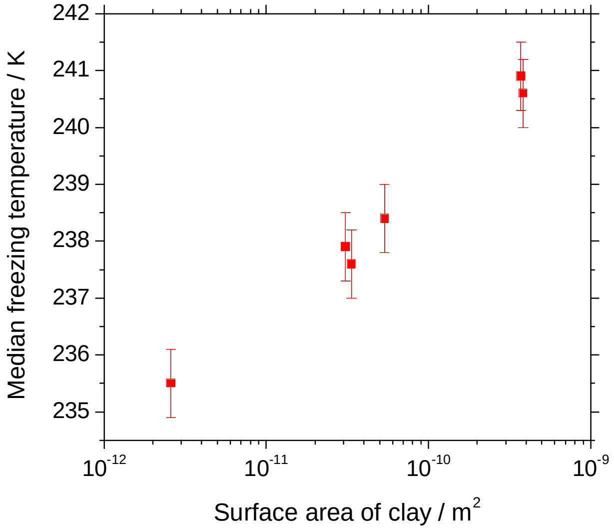

Fig. 2. The median freezing temperature (T_f) of a droplets containing varying amounts of kaolinite as a function of the surface area of kaolinite in a median sized droplet. The surface area of kaolinite inclusions was varied by changing the concentration of kaolinite suspended in water and the median volume of the droplets only varied within a factor of two.

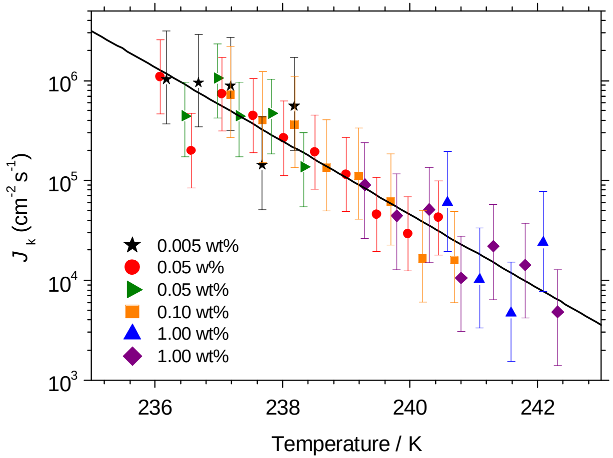

Fig. 3. Nucleation rates of ice on kaolinite in pure water expressed in units of $cm^{-2}\,s^{-1}$. The black line is a best fit to the data where $\ln J_k = -0.8484T + 214.3$, which is valid between 236 and 242.3 K. The vertical error bars were estimated based on the standard deviation in droplet volume and the specific surface area of the clay (see Table 1). The uncertainty in temperature was ±0.6 K.

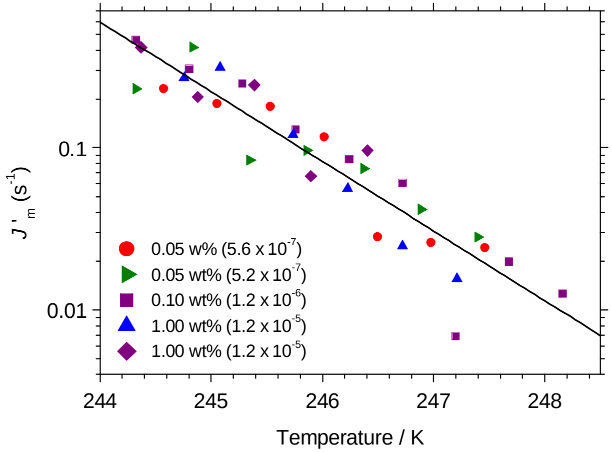

Fig. 4. Nucleation rate for montmorillonite expressed in units of s^{-1} (J'_m). Surface areas of montmorillonite per median sized droplet in cm^{-2} are indicated within brackets in the legend along with the wt% mineral. The solid line is a fit to the data where $\ln J'_m = -0.9897T + 241.0$. J'_m is only dependent on the number of droplets which froze in a certain time interval (Eq. 2) and the experimental uncertainties in both of these quantities were small, hence no vertical error bars are shown. The uncertainty in temperature was ±0.6 K.

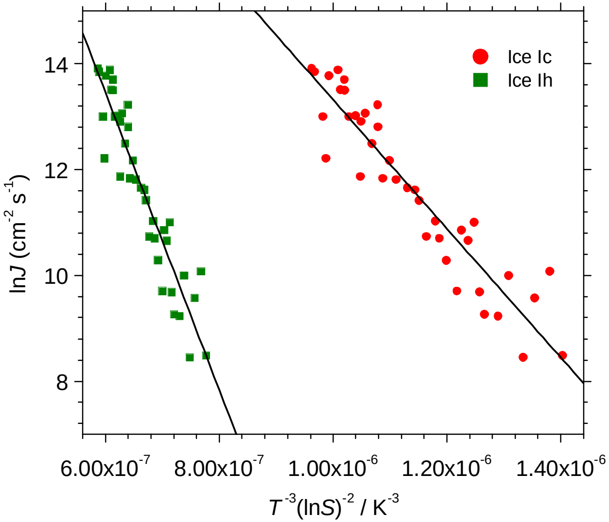

Fig. 5. Nucleation rate of ice on kaolinite as a function of $T^{-3}(\ln S_{\mathrm{Ic}})^{-2}$ (green squares) and $T^{-3}(\ln S_{\mathrm{Ih}})^{-2}$ (red circles). The fits to this data (solid line) yield ice nucleating efficiency parameters, m, for the two scenarios. See text for details.

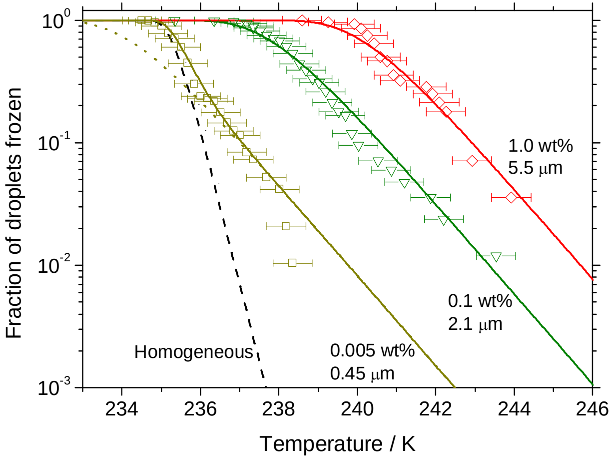

Fig. 6. Fraction of droplets frozen as a function of temperature for a range of kaolinite concentrations. Experimental data is compared with our parameterisation. The dotted line for the 0.005 wt% data is the fraction frozen if homogeneous nucleation is neglected, whereas the solid line is where both homogeneous and heterogeneous nucleation are included. The radius of a single spherical clay particle that has the same surface area as the particles within a median droplet in our experiments is also given.

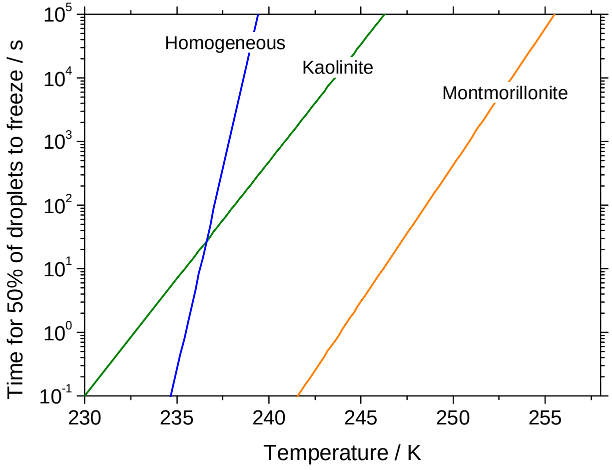

Fig. 7. The time required to freeze 50% of a population of droplets (t_{50}) as a function of temperature. The kaolinite line is for 1 µm diameter particles suspended in droplets (ignoring homogeneous nucleation) and the homogeneous line is for homogeneous nucleation in 20 µm diameter water droplets. Note that heterogeneous nucleation does not depend on droplet volume. The montmorillonite nucleation rate does not depend on particles size in the micrometer size range.

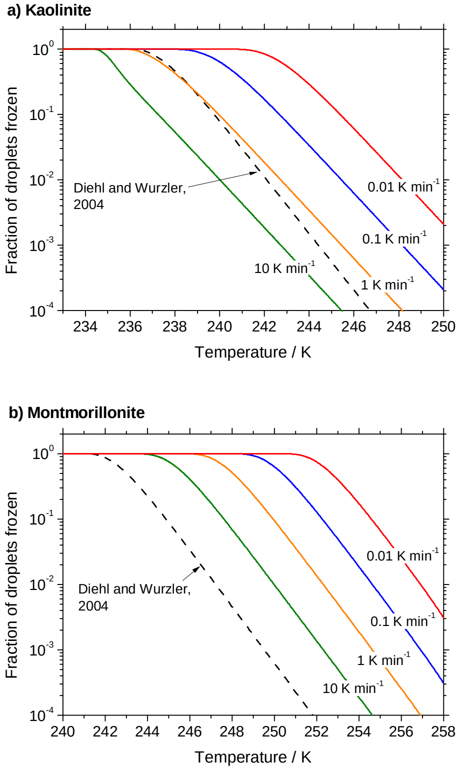

Fig. 8. Fraction of droplets frozen for a range of atmospherically relevant cooling rates for kaolinite and montmorillonite. These lines were calculated based on Eqs. (8) to (14). The kaolinite plot is for spherical kaolinite particles of 1 µm diameter immersed in water droplets of 20 µm diameter, whereas the rate of nucleation by montmorillonite is independent of surface area of particles in the micron size range. We have compared our cooling rate dependent parameterisation with that of Diehl and Wurzler (2004) for the same droplet sizes. Diehl and Wurzler's parameterisation neglects the cooling rate and the surface area dependence of heterogeneous ice nucleation.